Synchronization of droop-controlled microgrids with distributed rotational and electronic generation

Johannes Schiffer, Darina Goldin, Jörg Raisch, Tevfik Sezi

Abstract— We consider the problem of frequency synchronization and power sharing in a lossy droop-controlled autonomous microgrid with distributed rotational and electronic generation (MDREG). At first, we establish equivalence of the dynamics of a regulated synchronous generator and a droop-controlled inverter with low pass filter. We then give a necessary and sufficient condition for local synchronization of the microgrid by using ideas from graph theory and second order consensus algorithms. In addition, we show that sources in an MDREG can achieve a desired active power distribution via frequency droop control and provide synchronization conditions for a lossless microgrid as a special case. Our analysis is further validated via a simulation example of a lossy microgrid based on the CIGRE benchmark medium voltage distribution network.

I. INTRODUCTION

Motivated by environmental, political, economic and technological aspects, electric power systems worldwide are undergoing large changes due to an increasing amount of renewable energy sources. Since many of the latter are small-scale distributed generation units connected at the low (LV) and medium voltage (MV) levels via AC inverters, the power generation structure is moving from large, centralized plants to smaller, distributed generation (DG) units. Additionally, the physical characteristics of inverters largely differ from the characteristics of conventional electrical generators, i.e. synchronous generators (SGs), requiring different control approaches [1].

Therefore, new concepts and strategies to operate the electric power system that ensure a reliable and stable operation are needed. In this context, the microgrid concept has attracted increasing attention in recent years [2], [3] and has also been identified as a key component in future electrical networks [4]. It addresses these issues by gathering a combination of generation units, loads and energy storage elements at distribution level into a locally controllable system, which can be operated in a decentralized and completely isolated manner from the main transmission system. An autonomous or islanded microgrid is operated in the latter mode.

An important problem in microgrid operation is frequency synchronization while sharing the power demand among the different generation units. The problem of power sharing mainly addresses the following question: how should the different generation units in the network adjust their output power upon load changes to fulfill the demand while satisfying a desired power distribution? It is a requirement

to achieve these objectives in a decentralized way without communication among units, thereby allowing a plug-and-play-like operation [2].

A control solution widely used to tackle this problem in large power systems is droop control [5]. Under this approach, the current value of the rotational speed of each SG in the network is monitored locally to derive how much power each SG needs to provide. Since performance under droop control is satisfactory for large systems, this technique has been adapted to inverters [6], [7]. Stability analysis of droop-controlled inverter-based systems is usually carried out by means of detailed small-signal analysis as well as extensive simulations and experimental studies aiming to characterize an admissible range for the control gains for system stability. Recently, conditions for proportional power sharing and synchronization of lossless microgrids with first-order inverter models have been derived [8] by applying results of the theory of coupled oscillators.

So far, most research on stability and power sharing of microgrids has focused on purely inverter-based systems. However, from a practical consideration, most present and near-future applications concern networks of mixed generation structure including SGs and inverter-interfaced distributed resources. We will refer to such a system as a *microgrid with distributed rotational and electronic generation (MDREG)*. In MDREGs, SGs may for example be used in combination with diesel engines or gas turbines [9]. Stability and performance of such systems have not yet been much explored from a system theoretic point of view. In [10] and [11] MDREGs that consist of two inverters and one to two SGs are investigated via simulations complemented by a numerical small signal stability analysis.

We address this open problem by deriving analytic local synchronization conditions for an autonomous MDREG by means of graph theory and second order consensus algorithms for multi-agent systems. Second order consensus algorithms have been used to study synchronization of harmonic oscillators [12] and have recently also been applied to frequency restoration in conventional power systems [13].

The main contributions of this work are: first, we establish equivalence of the dynamics of a regulated SG and an inverter equipped with the typically proposed frequency droop control combined with a low pass filter, e.g. for power measurement [7]. Altough several authors have proposed to make inverters resemble the input/output behavior of SGs [14], [15], to the best of our knowledge, this observation has not been stated in the literature in a mathematically rigorous fashion to date. Second, we provide a necessary and sufficient local synchronization condition for a lossy MDREG, i.e. a MDREG with nonzero transfer conductances. The presence

J. Schiffer and D. Goldin are with the Technische Universität Berlin, Germany {schiffer,goldin}@control.tu-berlin.de

J. Raisch is with the Technische Universität Berlin & Max-Planck-Institut für Dynamik komplexer technischer Systeme, Germany raisch@control.tu-berlin.de

T. Sezi is with Siemens AG, Smart Grid Division, Nuremberg, Germany tevfik.sezi@siemens.com

of transfer conductances leads to non-symmetric network interconnections, complicating significantly the derivation of analytic stability conditions. Here, we do not make any assumptions on the power line characteristics nor the voltage levels, but assume uniform damping, as sometimes used in analysis of lossy conventional power systems [16]. Subsequently, we apply our results to derive synchronization conditions for lossless microgrids. In the latter case, the network interconnections are symmetric and we drop the assumption of uniform damping. We further indicate how a desired power distribution can be achieved in a synchronized state. Our analysis is validated in a simulation example based on the CIGRE benchmark MV distribution network [17].

II. PRELIMINARIES AND NOTATION

Let $x := \text{col}(x_i)_{\{i=1,\dots,n\}} \in \mathbb{R}^n$ denote an $n \times 1$ column vector with entries x_i, $\underline{1}_n$ denote the $n \times 1$ column vector of all ones, $\underline{0}_n$ denote the $n \times 1$ column vector of all zeros and $\text{diag}(a_i), i = 1,\dots n$ denote an $n \times n$ diagonal matrix with entries a_i. Let j denote the imaginary unit. The conjugate transpose of a vector v is denoted by v^*. We define the sets $\mathbb{R}^+ := \{x \in \mathbb{R} | x > 0\}$, $\mathbb{R}_0^+ := \{x \in \mathbb{R} | x \geq 0\}$, $\mathbb{R}^- := \{x \in \mathbb{R} | x < 0\}$ and $\mathbb{T} := [-\pi, \pi]$ with $-\pi$ and π identified. For a set $\mathcal{U} := \{\nu_1, \dots, \nu_n\}$, $i \sim \mathcal{U}$ denotes $i = \nu_1, \dots, \nu_n$.

A. Graph theory

This section provides a brief overview of graph theoretic notions employed in this paper. For further information, the reader is referred to, e.g. [18].

A weighted directed graph of order n is a 3-tuple $\mathcal{G} := (\mathcal{V}, \mathcal{E}, w)$, where $\mathcal{V} := \{1, \dots, n\}$ is the set of nodes, $\mathcal{E} \subseteq \mathcal{V} \times \mathcal{V}$ is the set of edges, i.e. ordered pairs of nodes (i, k) and $w : \mathcal{E} \to \mathbb{R}^+$ is a weight function.

Some notions associated with weighted directed graphs are the $|\mathcal{E}| \times |\mathcal{V}|$ incidence matrix $\mathcal{Q}$, the $|\mathcal{E}| \times |\mathcal{E}|$ diagonal matrix of edge weights $\mathcal{W}$ and the index set $\mathcal{I}$. Given an (arbitrary) ordering of the edges in the graph, each row of $\mathcal{Q}$ and each diagonal entry of $\mathcal{W}$ correspond to an edge of the graph. Namely $\mathcal{Q}_{li} = 1$ and $\mathcal{Q}_{lk} = -1$ if i is the initial and k the final node of the lth edge $e_l \in \mathcal{E}$ and $\mathcal{W}_{ll} = w(i, k)$, where $w(i, k)$ is the edge weight associated to e_l. Note that if there is an edge from i to k and an edge from k to i, then these two edges are described by two linearly dependent rows of $\mathcal{Q}$. The index set $\mathcal{I}$ has entries $\chi_m := (i, k)$, $m = 1, \dots, |\mathcal{E}|$ if there exists an edge from node i to node k.

We further use the $|\mathcal{V}| \times |\mathcal{E}|$ *orientation matrix* $\mathcal{C}$ with entries $\mathcal{C}_{ki} := 1$ if $\mathcal{Q}_{ik} = 1$ and 0 otherwise, introduced in [19]. With $\mathcal{C}$, the Laplacian matrix of a weighted directed graph with positive edge weights is given by

$$\mathcal{L} := \mathcal{C}\mathcal{W}\mathcal{Q}. \quad (1)$$

The diagonal entries of $\mathcal{L}$ are nonnegative, its off-diagonal entries are nonpositive and its row sums are 0.

A path between two nodes is a directed chain of edges. $\mathcal{G}$ is called strongly connected if for all $i, k \in \mathcal{V}$, there exists a path from i to k. Given a weighted directed graph, zero is a simple eigenvalue of its Laplacian $\mathcal{L}$ if the graph is strongly connected. All nonzero eigenvalues of $\mathcal{L}$ have a positive real part [18].

B. Electrical networks

Typically, a time-dependent phase angle $\delta_i : \mathbb{R}_0^+ \to \mathbb{T}$ and a voltage amplitude $E_i : \mathbb{R}_0^+ \to \mathbb{R}^+$ are associated to each node i in a power network. Furthermore, two nodes i and k are connected via a power line characterized by a complex admittance $\tilde{Y}_{ik} = \tilde{Y}_{ki} := \tilde{G}_{ik} + j\tilde{B}_{ik} \in \mathbb{C}$ with conductance $\tilde{G}_{ik} \in \mathbb{R}_0^+$ and susceptance $\tilde{B}_{ik} \in \mathbb{R}^-$. Usually in power system stability analysis, the power lines are assumed to be lossless, i.e. $\tilde{G}_{ik} = 0$ [5]. While this assumption is reasonable on the transmission level, it does not hold in general for a microgrid on the MV or LV level. We will therefore focus our analysis on the more general case of a lossy network, i.e. $\tilde{G}_{ik} \neq 0$, while treating the lossless network as a special case. We assume constant though not necessarily equal voltage amplitudes E_i throughout the paper. Then, constant power loads can equivalently be represented by constant impedance loads of the form $P_{L_i} := \tilde{G}_{ii}E_i^2$, where P_{L_i} denotes the active power consumed by the load at node i and $\tilde{G}_{ii}$ is a self-admittance. Nodes to which only such loads are connected are called passive nodes. A standard procedure in power system stability analysis is then to eliminate all passive nodes via the so-called Kron-reduction [5] leading to a lower dimensional representation of the original network in which all nodes represent generation units.

We assume that this process has been carried out and consider a model of a Kron-reduced lossy microgrid. This microgrid is formed by $n := n_1 + n_2$ nodes, of which $\mathcal{V}_I := \{1, \dots, n_1\}$ represent DG units interfaced via AC inverters and $\mathcal{V}_{SG} := \{(n_1 + 1), \dots, n\}$ are DG units interfaced via SGs. We denote the Kron-reduced network graph by $\mathcal{G}$, its set of nodes by $\mathcal{V} := (\mathcal{V}_I \cup \mathcal{V}_{SG})$ and its edge set by $\mathcal{E}$. To each node $i \in \mathcal{V}$ a phase angle $\delta_i(t)$ and a constant voltage amplitude $E_i \in \mathbb{R}^+$ are associated. We further assume that $\mathcal{G}$ is strongly connected. This assumption is reasonable for a microgrid, unless severe line outages separating the system into several disconnected parts occur.

For ease of notation, we will write angle differences as $\delta_{ik} := \delta_i - \delta_k$, whenever convenient. Further, we denote by $\omega_R \in \mathbb{R}^+$ the rated network frequency and express all internal frequencies $\hat{\omega}_i : \mathbb{R}_0^+ \to \mathbb{R}$ relative to a synchronously rotating reference frame with constant angular velocity ω_R

$$\dot{\delta}_i(t) := \omega_i(t) := \hat{\omega}_i(t) - \omega_R, \quad i \sim \mathcal{V}. \quad (2)$$

This is a common approach in power systems, see, e.g. [5], [20] for details. For convenience, we define the vectors $\delta(t) := \text{col}(\delta_i(t))_{\{i \sim \mathcal{V}\}}$ and $\omega(t) := \text{col}(\omega_i(t))_{\{i \sim \mathcal{V}\}}$.

The active power flow $P_{ik} : \mathbb{T}^2 \to \mathbb{R}$ from a node $i \in \mathcal{V}$ to a node $k \in \mathcal{V}$ is given by [5]

$$P_{ik}(t) = G_{ik}E_i^2 + |Y_{ik}|E_iE_k \sin(\delta_i(t) - \delta_k(t) + \phi_{ik}) \quad (3)$$

with admittance magnitude $|Y_{ik}| := \sqrt{G_{ik}^2 + B_{ik}^2}$ and admittance angle $\phi_{ik} := \arctan(G_{ik}/B_{ik})$. The overall active power flow $P_i : \mathbb{T}^n \to \mathbb{R}$ at a node $i \in \mathcal{V}$ is obtained by

$$P_i(t) = G_{ii}E_i^2 + \sum_{\substack{k=1, k \neq i \\ Y_{ik} \neq 0}}^{n} |Y_{ik}|E_iE_k \sin(\delta_i(t) - \delta_k(t) + \phi_{ik}) \quad (4)$$

with $G_{ii} := \hat{G}_{ii} + \sum_{k=1, k \neq i}^{n} G_{ik}$, where $\hat{G}_{ii}$ denotes the shunt conductance at node i. Since we are mainly concerned with dynamics of generation units, we express all power flows in "Generator Reference-Arrow System".

C. Synchronization

We employ the following definition of synchronization.

Definition 2.1: The microgrid achieves synchronization asymptotically if $\lim_{t\to\infty}|\omega_i - \omega_k| = 0$ and $\lim_{t\to\infty}|\delta_i - \delta_k| = |\delta^s_{ik}| \geq 0$, where $\delta^s_{ik} \neq \delta^s_{ik}(\delta(0), \omega(0))$ is constant for all $i, k = 1, \ldots, n$.
We denote the vector of angles of a synchronized solution by $\delta^s : \mathbb{R}^+_0 \to \mathbb{T}^n$ and the synchronization frequency by $\omega^s : \mathbb{R}^+_0 \to \mathbb{R}$.

D. Droop control

In a so-called regulated machine at a node $i \in \mathcal{V}_{SG}$, the turbine is connected to a governing system allowing to control the turbine mechanical power output $P_{M_i} : \mathbb{R}^+_0 \to \mathbb{R}$ and speed. These systems are usually equipped with *droop control*, which adapts the mechanical power in dependency of the turbine speed. Assuming a linear relationship between the valve position and the mechanical power as well as ideal governor dynamics and noting that the mechanical speed $\omega_{M_i} : \mathbb{R}^+_0 \to \mathbb{R}$ is connected to the electrical speed ω_i via $\omega_i = (p_i/2)\omega_{M_i}$ with p_i being the number of machine poles, droop control can be represented as $u_{G_i} : \mathbb{R}^+_0 \to \mathbb{R}$ [5], [21]

$$u_{G_i}(t) = P_{M_i}(t) = P^d_{M_i} - \frac{1}{\tilde{k}_{P_i}}\omega_i(t). \tag{5}$$

This is a proportional control law with input signal ω_i, gain $1/\tilde{k}_{P_i} \in \mathbb{R}^+$ and output P_{M_i}. The constant $P^d_{M_i} \in \mathbb{R}^+$ is the reference setpoint for the mechanical power.

Since droop control is a widely used control solution to address the problem of power sharing in large conventional power systems [5], researchers have proposed to also apply this technique to inverters. Opposed to an SG, an inverter does not have an inherent physical relation between frequency and generated active power. Frequency droop control aims at artificially creating such a relation via the control law [6], [7]

$$u_{I_i}(t) = \hat{\omega}_i(t) - \omega_R = -k_{P_i}(P^m_i(t) - P^d_i) \tag{6}$$

with $u_{I_i} : \mathbb{R}^+_0 \to \mathbb{R}$, $i \in \mathcal{V}_I$, droop gain $k_{P_i} \in \mathbb{R}^+$, measured active power $P^m_i : \mathbb{R}^+_0 \to \mathbb{R}$ and desired active power setpoint $P^d_i \in \mathbb{R}$. This is again a proportional control law, but now the input signal is the deviation in power $(P^m_i - P^d_i)$ and the output is the internal inverter frequency $\hat{\omega}_i$, the reference setpoint of which is the rated network frequency ω_R. Thus, from (2) we have $u_{I_i} = \omega_i$.

III. Modelling of an MDREG

Assuming that a droop-controlled *inverter* at a node $i \in \mathcal{V}_I$ is operated in voltage source mode and equipped with some sort of storage (e.g. flywheel, battery), it can increase and decrease its power output in a certain range. Then, an inverter with constant voltage amplitude and frequency droop control (6) can be modelled as [22]

$$\dot{\delta}_i(t) = u_{I_i}(t) = -k_{P_i}(P^m_i(t) - P^d_i),$$
$$\tau_{P_i}\dot{P}^m_i(t) = -P^m_i(t) + P_i(t), \tag{7}$$

where $\tau_{P_i} \in \mathbb{R}^+$ is the time constant of the low pass filter of the power measurement [7]. Since an inverter may connect a pure storage device, e.g. a battery, to the network, P^d_i can also take negative values. In that case, the storage device is charged in dependency of the excess power available in the network and thus functions as a frequency dependent load.

For the generator dynamics at a node $i \in \mathcal{V}_{SG}$, we consider the classical representation of a regulated *synchronous generator* by a constant voltage behind transient reactance together with the droop control law (5) [5], [21]. We denote by $M_i \in \mathbb{R}^+$ the inertia coefficient and by $D_i \in \mathbb{R}^+$ the damping term. Defining $k_{P_i} := \tilde{k}_{P_i}/(1 + \tilde{k}_{P_i}D_i)$, the regulated SG dynamics can be represented as

$$\dot{\delta}_i(t) = \omega_i(t),$$
$$M_i\dot{\omega}_i(t) = -\frac{1}{k_{P_i}}\omega_i(t) + P^d_{M_i} - P_i(t). \tag{8}$$

We further associate to each source its power rating $P^N_i \in \mathbb{R}^+$, $i \sim \mathcal{V}$. To simplify notation the time argument of all signals is omitted, whenever it is clear from the context, and we denote k_{P_i}, $i \sim \mathcal{V}$, as droop gains in the sequel.

IV. Synchronization and power sharing in an MDREG

We start our analysis by comparing the dynamics of a regulated SG and a frequency droop-controlled inverter, leading to the following observation.

Lemma 4.1: The dynamics of a frequency droop-controlled inverter (7) and a regulated SG (8) are equivalent.

Proof: For $i \in \mathcal{V}_I$, define the "virtual" inertia coefficient $M_i := \tau_{P_i}/k_{P_i}$, as well as $P^d_{M_i} := P^d_i$. Recall that $\dot{\delta}_i = \omega_i$. Differentiating ω_i in (7) with respect to time and using (7) to substitute P^m_i, we can rewrite (7) as

$$\dot{\delta}_i = \omega_i,$$
$$M_i\dot{\omega}_i = -\frac{1}{k_{P_i}}\omega_i + P^d_{M_i} - P_i. \tag{9}$$

∎

Remark 4.2: It follows from Lemma 4.1 that if one main control design intention for an inverter operated in voltage source mode is to achieve a behavior with respect to frequency similar to that of an SG, the rather simple structure given in (7) is sufficient and no additional components are required. Moreover, (9) reveals that the time constants τ_{P_i} of the low pass filters can be used as additional design parameters to shape the desired "virtual" inertia coefficients M_i of the inverters. Methods to emulate additional characteristics of SGs are proposed, e.g. in [14], [15].

For ease of notation, we are going to use (9) in the sequel to represent the inverter dynamics. We further define the matrices and column vectors

$$M := \text{diag}(M_i)_{\{i\sim\mathcal{V}\}}, \quad K := \text{diag}(1/k_{P_i})_{\{i\sim\mathcal{V}\}},$$
$$P^d_M := \text{col}(P^d_{M_i})_{\{i\sim\mathcal{V}\}}, \quad P := \text{col}(P_i)_{\{i\sim\mathcal{V}\}} \tag{10}$$

with power flows P_i given in (4). Then, the MDREG with node dynamics as in (8), (9) can be written compactly as

$$\dot{\delta}(t) = \omega(t),$$
$$M\dot{\omega}(t) = -K\omega(t) + P^d_M - P(t). \tag{11}$$

To state our main result, we need the following assumption on existence of a synchronized trajectory of system (11).

Assumption 4.3: There exist constants $\delta^s \in \Sigma$ and $\omega^s \in \mathbb{R}^+$ such that the system (11) possesses a synchronized solution

$$\delta^*(t) = \text{mod}_{2\pi}\{\delta^s + \underline{1}_n\omega^s t\}, \quad \omega^*(t) = \underline{1}_n\omega^s \tag{12}$$

for all $t \geq 0$, where the index set $\mathcal{I}$ is defined in II-A and $\Sigma := \{\delta^s \in \mathbb{T}^n \mid -\frac{\pi}{2} < \delta^s_{ik} + \phi_{ik} < \frac{\pi}{2} \text{ for all pairs } (i,k) \in \mathcal{I}\}$.

Remark 4.4: The power flows P in (10) are invariant to a uniform shift of all angles. Consequently, δ^* is only unique up to such a shift. To keep notation reasonably simple we will omit this non-uniqueness in the sequel.

A. Frequency synchronization in a lossy MDREG

A related work is [23], where under the assumption of small inertia over damping ratios, synchronization conditions for a nonlinear lossy power system with purely SGs have been derived. The microgrid (11) is very similar to the model used in [23]. The authors of [23] obtain their results via a singular perturbation approach that leads to reduced first-order dynamics of (11). For the model (11), the perturbation assumption of [23] reads $\epsilon := \max\left(\max_{i\sim\mathcal{V}_I}\tau_{P_i}, \max_{i\sim\mathcal{V}_{SG}}M_ik_{P_i}\right) \ll 1$.

Another assumption sometimes used in analysis of lossy power systems is uniform damping [16]. In our notation this assumption reads $\tau_{P_i} = \tau_{P_k} = \ldots = M_lk_{P_l} = M_mk_{P_m}$, $i, k \sim \mathcal{V}_I$, $l, m \sim \mathcal{V}_{SG}$. None of the two assumptions is valid for generic lossy power systems, see [23] and discussion therein. Since in the present case τ_{P_i} and k_{P_i} represent free design parameters, we can enforce the latter assumption for the synchronization analysis of a lossy MDREG. Further, we work with the local approximation of the full second order model (11) in the sequel. Then, we can use ideas from second order consensus theory to provide a necessary and sufficient condition for the droop gains $k_{P_i}, i \sim \mathcal{V}$ and low pass filter time constants $\tau_{P_i}, i \sim \mathcal{V}_I$ under which the synchronized solution defined in Assumption 4.3 is locally stable.

Assumption 4.5: The parameters $\tau_{P_i}, \tau_{P_k}, i, k \sim \mathcal{V}_I$, and $\tilde{k}_{P_l}, \tilde{k}_{P_m}, l, m \sim \mathcal{V}_{SG}$ are selected such that $\tau_P = \tau_{P_i} = \tau_{P_k} = \ldots = M_lk_{P_l} = M_mk_{P_m}$.

Remark 4.6: The droop gains of the inverters $k_{P_i}, i \sim \mathcal{V}_I$ are not restricted by Assumption 4.5.

Given a graph $\mathcal{G} = (\mathcal{V}, \mathcal{E}, w)$ induced by the microgrid, let $\mathcal{C}$ be its orientation matrix, $\mathcal{Q}$ its incidence matrix and $\mathcal{W}$ its diagonal matrix of edge weights, cf. II-A. The lth row of $\mathcal{Q}$ corresponds to the lth edge in $\mathcal{E}$, $l \in \{1, \ldots, |\mathcal{E}|\}$ given by (i, k), $i, k \in \{1, \ldots, n\}$. It represents the linearized synchronized power flow P_{ik}^s from node i to k as given in (3). Here, i is the initial node, k the final node and $\mathcal{W}_{ll} = w(i, k) = E_iE_k|Y_{ik}|\cos(\delta_{ik}^s + \phi_{ik})$ the edge weight.

Linearizing the vector of power flows P in (10) around a synchronized state with phase angle vector δ^s, we obtain

$$\left.\frac{\partial P}{\partial \delta}\right|_{\delta^s} := L = \mathcal{CWQ}. \tag{13}$$

It is easily verified that under Assumption 4.3 it holds that $\mathcal{W}_{ll} > 0, \forall l = 1, \ldots, |\mathcal{E}|$. Consequently, L is then a (non-symmetric) Laplacian matrix.

We define the deviations of the system variables with respect to the synchronized solution (12) as

$$\tilde{\omega}(t) := \omega(t) - \mathbb{1}_n\omega^s \in \mathbb{R}^n,$$
$$\tilde{\delta}(t) := \delta(0) - \delta^s + \int_0^t \tilde{\omega}(\tau)d\tau \in \mathbb{R}^n. \tag{14}$$

Then, under Assumption 4.5, the microgrid dynamics (11) can locally be modelled as a second order consensus system

$$\begin{bmatrix} \dot{\tilde{\delta}}(t) \\ \dot{\tilde{\omega}}(t) \end{bmatrix} = \underbrace{\begin{bmatrix} 0_{n\times n} & I_{n\times n} \\ -M^{-1}L & -\frac{1}{\tau_P}I_{n\times n} \end{bmatrix}}_{:=\mathcal{T}} \begin{bmatrix} \tilde{\delta}(t) \\ \tilde{\omega}(t) \end{bmatrix}. \tag{15}$$

We are now ready to state our main result.

Proposition 4.7: Consider the system (11) satisfying Assumptions 4.3 and 4.5. Let $\mu_i = a_i + jb_i$ be the ith eigenvalue of $M^{-1}L$, $i = 1, \ldots, n$. Then, the MDREG (11) achieves synchronization in a neighbourhood of (12) if and only if for all i with $a_i \neq 0$ and $b_i \neq 0$

$$\tau_P^2 < \frac{a_i}{b_i^2}. \tag{16}$$

Moreover, if $M^{-1}L$ has only real eigenvalues $\mu_i = a_i$, $i = 1, \ldots, n$, the MDREG (11) achieves synchronization in a neighbourhood of (12) for any τ_P.

Proof: We have just shown that with our assumptions, the microgrid (11) is locally equivalent to the system (15). The proof is thus given for system (15). It has been shown in [12] that $\lim_{t\to\infty}\tilde{\omega}_i(t) = 0$ and $\lim_{t\to\infty}|\tilde{\delta}_i(t) - \tilde{\delta}_k(t)| = 0$, for $i, k = 1, \ldots, n$ iff $\mathcal{T}$ has exactly one zero eigenvalue and all the other eigenvalues of $\mathcal{T}$ have negative real parts. We will thus prove Proposition 4.7 by deriving the spectrum of $\mathcal{T}$. The eigenvalues of $\mathcal{T}$ are the roots of

$$\det(\lambda I_{2n} - \mathcal{T}) = \det(P(\lambda)), \tag{17}$$

where $P(\lambda) = \lambda^2 I_n + \tau_P^{-1}\lambda I_n + M^{-1}L$. For any $v \in \mathbb{C}^n$ with $v^*v = 1$, we have

$$v^*P(\lambda)v = \lambda^2 + \tau_P^{-1}\lambda + v^*M^{-1}Lv. \tag{18}$$

Now, choose $v = v_i$, where v_i is a right eigenvector of $M^{-1}L$, i.e. $M^{-1}Lv_i = \mu_iv_i$, with $\mu_i \in \mathbb{C}$, $i = 1, \ldots, n$ being the eigenvalues of $M^{-1}L$. Then, (18) becomes

$$v_i^*P(\lambda)v_i = \lambda^2 + \tau_P^{-1}\lambda + \mu_i = 0 \tag{19}$$

and the eigenvalues of $\mathcal{T}$ are the solutions $\lambda_{i_{1,2}}$ of

$$\lambda_i^2 + \tau_P^{-1}\lambda_i + \mu_i = 0, \quad i = 1, \ldots, n. \tag{20}$$

As M is diagonal, $M^{-1}L$ is a Laplacian for $\delta^s \in \Sigma$ and has exactly one zero eigenvalue, since $\mathcal{G}$ is strongly connected by assumption. We let $\mu_1 = 0$. All the other eigenvalues μ_i, $i = 2, \ldots, n$ have positive real parts.

For $\mu_1 = 0$, (20) has solutions $\lambda_{1_1} = 0$, $\lambda_{1_2} = -1/\tau_P$. It remains to show that all solutions $\lambda_{i_{1,2}}$, $i = 2, \ldots, n$ of (20) have negative real parts. First, consider real nonzero eigenvalues, i.e. $\mu_i = a_i$ with $a_i > 0$. Then, clearly, both solutions of (20) have negative real parts, e.g. by the Hurwitz condition. Next, consider complex eigenvalues, i.e. $\mu_i = a_i + jb_i$, $a_i > 0, b_i \in \mathbb{R}\setminus\{0\}$. Then, from (20) we have

$$\lambda_{i_{1,2}} = \frac{1}{2\tau_P}\left(-1 \pm \sqrt{1 - 4\tau_P^2(a_i + jb_i)}\right). \tag{21}$$

We define $\alpha_i := 1 - 4a_i\tau_P^2$, $\beta_i := -4b_i\tau_P^2$ and recall that the roots of a complex number $\sqrt{\alpha_i + j\beta_i}, \beta_i \neq 0$ are given by $\pm(\psi_i + j\nu_i)$ [24] with

$$\psi_i = \sqrt{\frac{1}{2}\left(\alpha_i + \sqrt{\alpha_i^2 + \beta_i^2}\right)}. \tag{22}$$

Thus, both solutions $\lambda_{i_{1,2}}$ in (21) have negative real parts iff

$$\sqrt{\frac{1}{2}\left(\alpha_i + \sqrt{\alpha_i^2 + \beta_i^2}\right)} < 1 \Leftrightarrow \sqrt{\alpha_i^2 + \beta_i^2} < 2 - \alpha_i. \tag{23}$$

Inserting α_i and β_i gives

$$\sqrt{(1 - 4a_i\tau_P^2)^2 + 16b_i^2\tau_P^4} < 1 + 4a_i\tau_P^2, \tag{24}$$

where the right hand side is positive. The condition is therefore equivalent to the claimed condition (16). ∎

B. Frequency synchronization in a lossless MDREG

A lossless microgrid with inductive lines and second order dynamics is obtained from (11) by setting $G_{ik} = 0$, respectively $\phi_{ik} = 0$ for all $i, k = 1, \ldots, n$.

Assumption 4.8: $G_{ik} = 0$ for all $i, k \in \mathcal{V}$.

Under Assumption 4.8, all loads present in the network are storage devices in charging mode, i.e. $P_{M_i}^d < 0$ for some $i = 1, \ldots, n_1$. The microgrid dynamics (11) can locally be modelled as the second order consensus system

$$\begin{bmatrix} \dot{\tilde{\delta}}(t) \\ \dot{\tilde{\omega}}(t) \end{bmatrix} = \underbrace{\begin{bmatrix} 0_{n \times n} & I_{n \times n} \\ -M^{-1}L & -M^{-1}K \end{bmatrix}}_{:= \mathcal{R}} \begin{bmatrix} \tilde{\delta}(t) \\ \tilde{\omega}(t) \end{bmatrix} \quad (25)$$

with L as defined in (13). Local synchronization follows as a corollary to Proposition 4.7.

Corollary 4.9: Consider the system (11) satisfying Assumptions 4.3 and 4.8. Then, the MDREG (11) achieves synchronization in a neighbourhood of (12) for arbitrary choices of k_{P_i}, $i = 1, \ldots, n$ and $\tau_{P_i}, i = 1, \ldots, n_1$.

Remark 4.10: We do not need Assumption 4.5 to prove synchronization in a lossless network, since L is a symmetric Laplacian matrix if $\delta^s \in \Sigma$ and $\phi_{ik} = 0$ for all $i, k \in \mathcal{V}$.

Proof: To show the corollary, we need to show that $\mathcal{R}$ possesses exactly one zero eigenvalue and that all other eigenvalues have negative real parts. To see this, observe that the eigenvalues of $\mathcal{R}$ are the roots of $\det(M^{-1}) \det(P'(\lambda))$ with $P'(\lambda) = \lambda^2 M + \lambda K + L$. Recall that M is a diagonal matrix with positive entries and that under Assumption 4.8 L is a symmetric Laplacian matrix of a strongly connected graph. Thus, L has exactly one zero eigenvalue and $n - 1$ positive real eigenvalues. Further, $v^* L v \geq 0$ for any vector $v \in \mathbb{C}^n$ with $v^* v = 1$. Now, choose $v = v_i$, where v_i, $i = 1, \ldots, n$ is a right eigenvector of $P'(\lambda)$, i.e. $P'(\lambda_0) v_i = 0$, for some eigenvalue $\lambda_0 \in \mathbb{C}$. Then

$$v_i^* P'(\lambda_0) v_i = 0 = \lambda_0^2 v_i^* M v_i + \lambda_0 v_i^* K v_i + v_i^* L v_i \quad (26)$$

and the solutions $\lambda_{0_{1,2}}$ of (26) are the eigenvalues of $\mathcal{R}$. Since $v_i^* M v_i$ and $v_i^* K v_i$ are positive real, the result follows by the Hurwitz condition. Local synchronization of (15) is concluded by Proposition 4.7. ∎

C. Power sharing

We next show how the droop control laws defined in (5) and (6) serve to achieve a desired power distribution among the generation units in a synchronized network state.

Lemma 4.11: Consider the microgrid (11) satisfying Assumption 4.3. Then, the generation units share the power in proportion to their power ratings P_i^N if the gains k_{P_i} and setpoints $P_{M_i}^d$ are chosen such that for all $i, k = 1, \ldots, n$

$$k_{P_i} P_{M_i}^d = k_{P_k} P_{M_k}^d \quad \text{and} \quad P_{M_i}^d / P_i^N = P_{M_k}^d / P_k^N. \quad (27)$$

Proof: The proof has been given for first-order droop-controlled inverters in [8] and carries over in a straightforward manner to the case of an MDREG with droop control laws as given in (5) and (6). Under conditions (27), we have along the synchronized trajectory defined in Assumption 4.3

$$\frac{P_i^s}{P_i^N} = \frac{P_{M_i}^d - k_{P_i}^{-1} \omega^s}{P_i^N} = \frac{P_{M_k}^d - k_{P_k}^{-1} \omega^s}{P_k^N} = \frac{P_k^s}{P_k^N}. \quad (28)$$

∎

Remark 4.12: Condition (28) holds for arbitrary line admittances. Hence, the MDREG (11) achieves proportional active power sharing in a synchronized state independently of the power line characteristics. However, in a highly ohmic network the droop control laws (5), (6) may induce high fluctuating currents due to the stronger coupling of phase angles and reactive power. Then, additional methods such as the virtual output impedance [25] or alternative droops [26] could be employed.

Remark 4.13: Under Assumption 4.5, proportional power sharing among generation units can be achieved via Lemma 4.11 if $M_k/M_i = P_k^N/P_i^N$ holds for all $i, k \sim \mathcal{V}_{SG}$.

V. SIMULATION EXAMPLE

To illustrate our theoretical analysis, we provide a simulation example for a lossy MDREG based on the inner ring of the islanded Subnetwork 1 of the CIGRE benchmark medium voltage distribution network [17]. The network consists of eight main buses and is shown in Fig. 1. The loads at buses 3, 4 and 8 to 11 (indicated by ↓) represent industrial and household loads. The non-controllable generation units are composed of photovoltaic plants (PV) at buses 3, 4, respectively 8 to 11. The four controllable electronic generation sources are a combined heat and power (CHP) fuel cell (FC) at bus 9b ($i = 1$), a battery (Bat) at bus 10b ($i = 2$), a fuel cell (FC) in a household at bus 10c ($i = 3$), as well as CHP diesel plant with SG at bus 9c ($i = 4$). Besides the diesel plant all controllable sources are interfaced via AC inverters to the network. The source numbering is as defined in II-B.

To permit an islanded operation of the system, the power ratings of the generation units are scaled by a factor 5 compared to [17], such that the controllable sources (CHPs, battery, FC) can satisfy the load demand in an autonomous operation mode at least during some period of time. The load data is as given in [17], besides the load at node 1, which is neglected. The line parameters and lengths are as given in [17]. The transformers of the sources are modelled with $R_{T_i} = 0.008 P_{\text{base}}/P_i^N$ pu, $X_{T_i} = 0.04 P_{\text{base}}/P_i^N$ pu, $i \in \mathcal{V}$, where pu denotes per unit values with respect to the common system base power P_{base} given in Table I. We assume for simplicity that the transformer power rating is equivalent to that of the corresponding generation source. The output filter inductances are assumed equal to $X_{F_i} = 0.0003$ pu, $i \in \mathcal{V}_I$. The simulations are carried out in Plecs [27].

We consider the following scenario: all PV units provide 50% of their rated power. The remaining power demand of the network (0.865 pu) should be supplied by the droop-controlled sources. The droop gains k_{P_i} and power setpoints $P_{M_i}^d$, $i = 1, \ldots, 4$ are designed following Lemma 4.11, i.e. such that the power is shared by the sources according to their ratings. Moreover, $\sum_{i=1}^4 P_{M_i}^d = 0.857$ pu. Since additionally the losses over lines are not considered explicitly in the selection of $P_{M_i}^d$, the microgrid is expected to synchronize close, but not exactly at nominal frequency.

Local stability is analyzed via Proposition 4.7. We therefore compute the equivalent Kron-reduced network of the microgrid in Fig. 1. In the present case, $M^{-1}L$ with L as defined in (13) has only real eigenvalues at the chosen equilibrium point. Thus, by Proposition 4.7, the microgrid synchronizes for initial conditions around the desired oper-
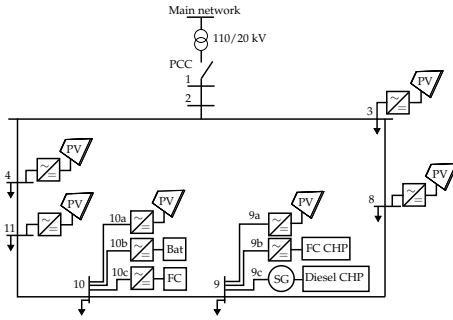
Fig. 1. 20 kV MV benchmark model adapted from [17] with eight main buses and generation sources of type: PV-Photovoltaic, FC-fuel cell, Bat-battery, CHP diesel, CHP fuel cell. The symbol ↓ denotes a load and PCC denotes the point of common coupling to the main grid.

TABLE I

TEST SYSTEM PARAMETERS

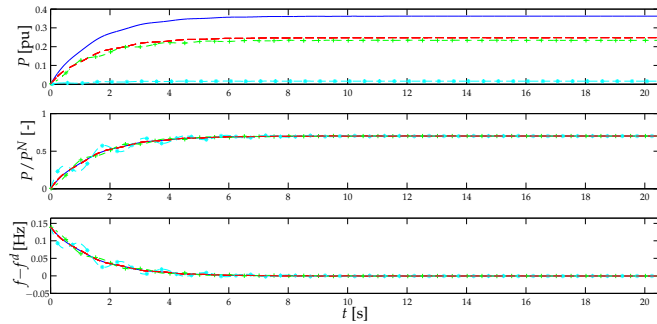| Base values	$P_{\text{base}} = 3$ MW, $V_{\text{base}} = 20$ kV
Max. system load	0.99 pu
Total nominal PV gen.	0.25 pu
SG data	$M_4 = 0.6064$ pu/Hz^2, $D_4 = 0$ pu/Hz
$P_i^N, i = 1, \ldots, 4$	[0.353, 0.333, 0.023, 0.517] pu
$P_{M_i}^d, i = 1, \ldots, 4$	[0.247, 0.233, 0.016, 0.361] pu
$k_{P_i}, i = 1, \ldots, 4$	[0.566, 0.600, 8.571, 0.387] Hz/pu

Fig. 2. Trajectories of absolute power outputs P_i in pu, power outputs relative to source ratings P_i/P_i^N and internal relative frequencies $f_i - f^d = \omega_i/(2\pi)$ in Hz of the controllable sources in the microgrid given in Fig. 2. The lines correspond to: FC CHP $i = 1$ '- -', battery $i = 2$ '- +', FC $i = 3$ '-*', SG diesel CHP $i = 4$ '–'.

ating point if Assumption 4.5 holds. Since only one SG is present in the network, Assumption 4.5 does not represent a major limitation. This holds especially for the proportional power sharing among sources. The main system data is given in Table I. All other system parameters are given in [17].

The simulation results are shown in Fig. 2. After a transient the frequencies synchronize close to the nominal frequency and the load of 0.865 pu is shared by the different sources in proportion to their ratings as derived in Lemma 4.11. The initial conditions have been chosen arbitrarily. The generation source $i = 3$ with smallest power rating P_i^N and consequently highest droop gain k_{P_i} (if designed according to Lemma 4.11) exhibits the largest internal frequency oscillations during the transient.

VI. CONCLUSION

Microgrids represent a promising near-time concept to facilitate increasing integration of distributed renewable sources. Opposed to most previous work, we have considered the general and practically very relevant case of a microgrid with mixed distributed rotational and electronic generation.

Furthermore, our analysis has addressed generic (possibly meshed) lossy networks, i.e. with nonzero transfer conductances, while treating lossless microgrids as a special case. We have provided conditions to guarantee local frequency synchronization and power sharing in such networks, when the generation units are operated with frequency droop control. Future research will consider relaxing the assumption on identical low pass filter time constants, as well as extending the analysis to time-dependent voltages and reactive power-voltage droops.

REFERENCES

[1] T. Green and M. Prodanovic, "Control of inverter-based micro-grids," *Elec. Power Sys. Research*, vol. Vol. 77, no. 9, pp. 1204–1213, 2007.
[2] R. Lasseter, "Microgrids," in *IEEE PSGM*, 2002, pp. 305 – 308.
[3] N. Hatziargyriou, H. Asano, R. Iravani, and C. Marnay, "Microgrids," *IEEE Power and Energy Magazine*, vol. 5, no. 4, pp. 78 –94, 2007.
[4] H. Farhangi, "The path of the smart grid," *IEEE Power and Energy Magazine*, vol. 8, no. 1, pp. 18 –28, 2010.
[5] P. Kundur, *Power system stability and control*. McGraw-Hill, 1994.
[6] M. Chandorkar, D. Divan, and R. Adapa, "Control of parallel connected inverters in standalone AC supply systems," *IEEE Trans. on Industry Applications*, vol. 29, no. 1, pp. 136 –143, 1993.
[7] E. Coelho, P. Cortizo, and P. Garcia, "Small-signal stability for parallel-connected inverters in stand-alone AC supply systems," *IEEE Trans. on Industry Applications*, vol. 38, no. 2, pp. 533 –542, 2002.
[8] J. W. Simpson-Porco, F. Dörfler, and F. Bullo, "Synchronization and power sharing for droop-controlled inverters in islanded microgrids," *Automatica*, vol. 49, no. 9, pp. 2603 – 2611, 2013.
[9] S. Krishnamurthy, T. Jahns, and R. Lasseter, "The operation of diesel gensets in a CERTS microgrid," in *IEEE PESGM-Conversion and Delivery of Electrical Energy in the 21st Century*, 2008, pp. 1 –8.
[10] F. Katiraei and M. Iravani, "Power management strategies for a microgrid with multiple distributed generation units," *IEEE Trans. on Power Systems*, vol. 21, no. 4, pp. 1821 –1831, 2006.
[11] Z. Miao, A. Domijan, and L. Fan, "Investigation of microgrids with both inverter interfaced and direct AC-connected distributed energy resources," *IEEE Trans. on Power Delivery*, vol. 26, no. 3, pp. 1634 –1642, 2011.
[12] W. Ren, "Synchronization of coupled harmonic oscillators with local interaction," *Automatica*, vol. 44, no. 12, pp. 3195 – 3200, 2008.
[13] M. Andreasson, H. Sandberg, D. V. Dimarogonas, and K. H. Johansson, "Distributed integral action: Stability analysis and frequency control of power systems," in *Proc. 51st IEEE CDC*, HI,USA, 2012.
[14] H.-P. Beck and R. Hesse, "Virtual synchronous machine," in *9th Int. Conf. on Electr. Power Quality and Utilisation*, 2007, pp. 1 –6.
[15] Q. Zhong and G. Weiss, "Synchronverters: Inverters that mimic synchronous generators," *IEEE Trans. on Industrial Electronics*, vol. 58, no. 4, pp. 1259 –1267, 2011.
[16] H.-D. Chiang, F. Wu, and P. Varaiya, "A BCU method for direct analysis of power system transient stability," *IEEE Trans. on Power Systems*, vol. 9, no. 3, pp. 1194 –1208, 1994.
[17] K. Rudion, A. Orths, Z. Styczynski, and K. Strunz, "Design of benchmark of medium voltage distribution network for investigation of DG integration," in *IEEE PESGM*, 2006, p. 6.
[18] C. Godsil and G. Royle, *Algebraic Graph Theory*. Springer, 2001.
[19] D. Goldin and J. Raisch, "On the weight controllability of consensus algorithms," in *Proc. ECC*, Zurich, Switzerland, 2013.
[20] P. Anderson and A. Fouad, *Power System Control and Stability*. J.Wiley & Sons, 2002.
[21] J. Machowski, J. Bialek, and J. Bumby, *Power system dynamics: stability and control*. J.Wiley & Sons, 2008.
[22] J. Schiffer, A. Anta, T. D. Trung, J. Raisch, and T. Sezi, "On power sharing and stability in autonomous inverter-based microgrids," in *Proc. 51st IEEE CDC*, HI, USA, 2012.
[23] F. Dörfler and F. Bullo, "Synchronization and transient stability in power networks and non-uniform Kuramoto oscillators," *SIAM Journal on Control and Optimization*, vol. 50, no. 3, pp. 1616–1642, 2012.
[24] S. Rabinowitz, "How to find the square root of a complex number," *Mathematics and Informatics Quarterly*, vol. 3, pp. 54–56, 1993.
[25] J. Guerrero, L. Garcia de Vicuna, J. Matas, M. Castilla, and J. Miret, "Output impedance design of parallel-connected UPS inverters with wireless load-sharing control," *IEEE Trans. on Industrial Electronics*, vol. 52, no. 4, pp. 1126 – 1135, 2005.
[26] Q.-C. Zhong, "Robust droop controller for accurate proportional load sharing among inverters operated in parallel," *IEEE Trans. on Industrial Electronics*, vol. 60, no. 4, pp. 1281–1290, 2013.
[27] Plexim GmbH, "Plecs software, www.plexim.com," 2013.